

9-27-2020

A study of water content distribution and shallow stability of earth slopes subject to rainfall infiltration

Zhen-ning SHI

National Engineering Laboratory of Highway Maintenance Technology, Changsha University of Science & Technology, Changsha, Hunan 410114, China

Shuang-xing QI

School of Civil Engineering, Changsha University of Science & Technology, Changsha, Hunan 410114, China

Hong-yuan FU

School of Traffic & Transportation Engineering, Changsha University of Science & Technology, Changsha, Hunan 410114, China

Ling ZENG

School of Civil Engineering, Changsha University of Science & Technology, Changsha, Hunan 410114, China

See next page for additional authors

Follow this and additional works at: <https://rocksoilmech.researchcommons.org/journal>



Part of the [Geotechnical Engineering Commons](#)

Custom Citation

SHI Zhen-ning, QI Shuang-xing, FU Hong-yuan, ZENG Ling, HE Zhong-ming, FANG Rui-min, . A study of water content distribution and shallow stability of earth slopes subject to rainfall infiltration[J]. Rock and Soil Mechanics, 2020, 41(3): 980-988.

This Article is brought to you for free and open access by Rock and Soil Mechanics. It has been accepted for inclusion in Rock and Soil Mechanics by an authorized editor of Rock and Soil Mechanics.

A study of water content distribution and shallow stability of earth slopes subject to rainfall infiltration

Authors

Zhen-ning SHI, Shuang-xing QI, Hong-yuan FU, Ling ZENG, Zhong-ming HE, and Rui-min FANG

A study of water content distribution and shallow stability of earth slopes subject to rainfall infiltration

SHI Zhen-ning^{1,2}, QI Shuang-xing³, FU Hong-yuan¹, ZENG Ling³, HE Zhong-ming¹, FANG Rui-min¹

1. School of Traffic & Transportation Engineering, Changsha University of Science & Technology, Changsha, Hunan 410114, China

2. National Engineering Laboratory of Highway Maintenance Technology, Changsha University of Science & Technology, Changsha, Hunan 410114, China

3. School of Civil Engineering, Changsha University of Science & Technology, Changsha, Hunan 410114, China

Abstract: A rainfall infiltration test model which enables the measurement of the volumetric water content of soil is designed. The distribution and variation of the initial water content under rainfall infiltration are obtained through the test. Based on these results, a novel method for shallow stability analysis of earth slopes subject to rainfall infiltration is proposed by combining the unsaturated shear strength theory and the limit equilibrium method. The proposed method is then applied to study the stability of a soil slope along the Qili connecting line of Hang-Xin-Jing Expressway. The main findings are as follows: The inverse proportion function characterized by water content distribution parameter A , correction coefficients λ and μ can be used to describe the initial water content distribution of soil in natural state. With the increase of A value, the initial stability of the slope decreases, and the sensitivity of rainfall to slope instability also decreases. When the rainfall intensity is the same, the greater the initial surface water content, the shorter the rainfall time needed to cause the slope instability, and when rainfall time is the same, the greater the initial surface water content, the smaller the rainfall intensity needed to cause the slope instability. Under the same groundwater level, the rainfall intensity is inversely proportional to the rainfall time needed to cause the slope instability.

Keywords: rainfall infiltration; soil slope; water content distribution; slope stability; rainfall intensity-duration curve

1 Introduction

There are many earth slopes being formed with engineering constructions in the mountainous and hilly areas. The failure of earth slopes often induce serious damage to the engineering projects, and even endanger the safety of human life and property^[1-2]. Statistical data show that most of the slope instability is directly caused by rainfall, such as shallow soil landslide in Nanjiang County^[3], accumulative landslide in Dashuchang Town, Three Gorges^[4], etc. It can be seen that rainfall infiltration is one of the most important causes of earth slope instability.

Increase of soil unit weight, reduction of soil shear strength, and the increase of pore water pressure caused by the rainfall infiltration or changes in the groundwater level are the main factors leading to the decrease of the stability of the earth slope^[5-7]. Thus, carrying out research on the slope internal water content distribution under rainfall infiltration is a prerequisite for the correct calculation of the slope stability. In this regard, many investigators have conducted a lot of researches from different aspects, and have drawn many useful conclusions. From the perspective of experimental research, Shi et al.^[8] designed a large-scale slope model and corollary rainfall system, and studied the sliding mechanism of the colluvial slope. They concluded that the increase in pore water pressure

in the soil caused by rainfall is one of the important reasons of slope instability. The research results of Zuo et al.^[9] showed that the downward movement of the wetting front has significant influence on the pore water pressure and the matric suction of the earth slope. From the perspective of numerical calculation and analysis, Tian et al.^[10] modified the rainfall infiltration boundary based on the Richard equation, and realized a simplified numerical simulation method of rainfall infiltration considering runoff replenishment. Wang et al.^[11] derived a rainfall infiltration function for landslides based on the Green-Ampt model, and described the expansion process of the wet front. Cuomo et al.^[12] conducted a seepage simulation on soils with different soil-water characteristics curves, and concluded that the soil-water characteristics curves would significantly influence the seepage process inside the slope. It can be seen that most of the existing studies are carried out from the perspective of rainfall-triggered slope instability mechanism and the modification of the original infiltration calculation method, and assume the original water content is uniformly distributed in elevation when analyzing the initial water content of the slope. The initial water content distribution inside the slope under different conditions is not considered.

Based on above discussions, there is an urgent need to study the internal water content distribution of the slope under

Received: 8 March 2019

Revised: 31 July 2019

This work was supported by the National Natural Science Foundation of China(51908069, 51978084, 51838001, 51878070), the Open Fund of National Engineering Laboratory of Highway Maintenance Technology (Changsha University of Science & Technology) (kfj170103), and the Key Research and Development Program of Hunan Province(2019SK2171).

First author: SHI Zhen-ning, male, born in 1990, PhD, Lecturer, research interests: slope stability. E-mail: shizhenning@126.com

different conditions, and further study the impact of rainfall infiltration on the slope stability. This study firstly carried out an one-dimensional rainfall infiltration indoor model test. According to the test results, the soil water content distribution model is obtained. Then, the slope stability changes under different groundwater levels and rainfall conditions are analyzed. The obtained results can provide a theoretical basis for the study of slope stability changes under rainfall infiltration and provide guidance for the design of slope drainage facilities.

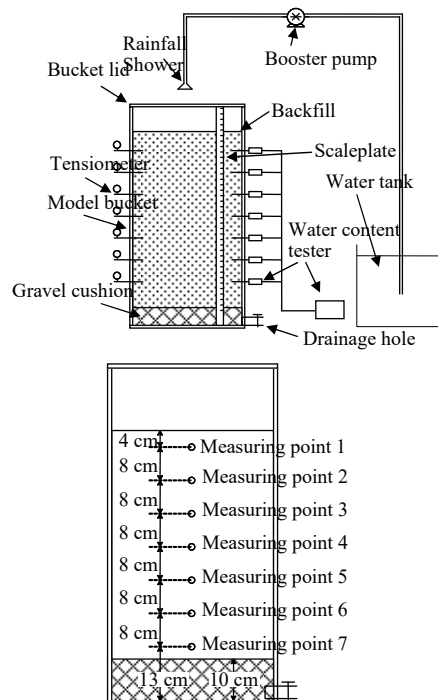
2 Rainfall infiltration model test

2.1 Test device and test process

To better understand the distribution characteristics of the internal water content of the soil along the elevation under rainfall infiltration, an indoor model test was carried out. The test device is shown in Fig.1. The diameter of the plexiglass



(a) Rainfall infiltration test model



(b) Schematic diagram of rainfall infiltration test model

Fig.1 Schematic diagram of the rainfall infiltration test model

tube is 40 cm, the wall thickness is 5 mm, the height is 80 cm, and the bottom crushed stone thickness is 10 cm. Drainage holes are made at the gravel cushion to control the groundwater level. The lowermost water content measuring point is 13 cm from the bottom of the barrel, and the measuring points are set at intervals of 8 cm upwards. The amount of backfill is calculated according to the dry density of the in-situ soil, and the backfill is compacted in layers to simulate the undisturbed soil. Before the test, the soil in the model bucket was saturated by simulating rainfall. The bucket lid was covered to prevent the evaporation of water. Then, the drainage hole at the bottom of the model bucket was opened to allow the water in the soil to naturally seep to the gravel cushion. When the water content distribution keeps stable along the elevation, the water content gauge is used for data collection to obtain the soil water content distribution. When carrying out the rainfall test, the booster pump was turned on. The water was then sprayed evenly on the soil according to the rainfall setups, and the drainage hole was closed at the same time, and the water content data was collected regularly to observe the change of the soil water content. The soil used in this test was silty clay sampled at the sliding surface of a cutting slope of the Qili connecting line of Hangxinjing Expressway. The soil property parameters and test design are shown in Table 1. No soil settlement was found during the test, and it can be considered that the parameters such as the void ratio keeps unchanged during the test.

2.2 Analysis of test results

Figure 2 shows the distribution characteristics of soil water content in the initial state and under the rainfall infiltration condition. In the initial state, the water content of the soil surface at the measuring point 1 was 23.9%, the water contents at the measuring points 2 to 5 were all around 25%, and the water contents at the measuring points 6 and 7 were 36.2% and 48.6%, respectively. It can be seen that as the height of the measuring point decreases, the water content continues to increase and the bottom of the soil is almost saturated. Then, the rain infiltration test was carried out on the basis of the initial water content distribution. When the rainfall time was 40 minutes, the water content at the measuring point 1 increased to 40.2%; when the rainfall time was 60 minutes, the water content at the measuring point 1 remained unchanged, and the water contents at the measuring points 2 and 3 increased to 38.1% and 34.4%, respectively. When the rainfall time reached 80 minutes, the water content of the measurement points 1 to 3 all increased to about 40%. When the rainfall time exceeds 120 minutes, the groundwater level began to rise gradually until the model was saturated.

The above test results suggest that the soil water content

Table 1 Soil parameters and the test condition

Soil type	Void ratio	Saturated water content	Particle diameter / (mm)	Saturated infiltration coefficient / (m · s ⁻¹)	Rainfall intensity / (m · s ⁻¹)	Rainfall duration / min	Observation frequency / (times/min)
Silty clay	1.041	0.51	< 2	7.37×10 ⁻⁵	1.3×10 ⁻⁵	260	20

during the rainfall infiltration changes as follows: in the initial state, the surface water content of the soil body is lower, and the water content near the groundwater level is higher. It can be considered that the water content generally has an inverse proportional relationship with the elevation. In the state of rainfall infiltration, the surface water content of the soil increases, and then the internal water content of the soil increases sequentially from top to bottom (stage 1 shown in Fig.2). When the rainfall infiltration reaches the bottom, the bottom soil water content continues to increase to saturation (stage 2 shown in Fig.2), and finally the water level gradually rises from bottom to top (stage 3 shown in Fig.2).

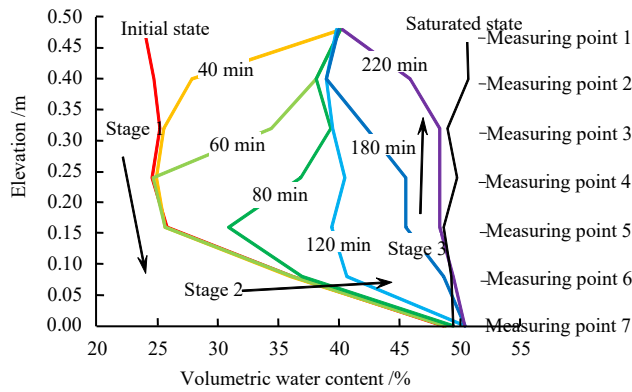


Fig.2 Rainfall-induced water content distribution of silty clay along the vertical direction

3 Distribution model of soil water content

3.1 Inverse proportional distribution model of initial water content

Based on the above test result analysis, the inverse proportional function model that describes the distribution characteristics of the initial water content of the soil along the elevation is

$$h = \frac{A}{\theta - B + \lambda} + h_w - \mu; \theta \in [B, \theta_s] \quad h_w \in [0, H] \quad (1)$$

where h is the height; θ is the volumetric water content; A is the water content distribution parameter; B is the soil water retention capacity (soil surface water content in natural state); h_w is the height of groundwater; θ_s is the saturated water content; H is the total height of the soil; λ and μ are the correction coefficients:

$$\lambda = \frac{\sqrt{(\theta_s - B)^2 + 4K} - (\theta_s - B)}{2} \quad (2)$$

$$K = \frac{(\theta_s - B)A}{H - h_w} \quad (3)$$

$$\mu = \frac{A}{\theta_s - B + \alpha} \quad (4)$$

where α is the control parameter of soil water characteristic curve.

Figures 3 and 4 show the effects of different water content distribution parameters (A value) and different groundwater levels on soil water content distribution when the saturated water content, surface water content, and soil height are constant. As can be seen from Fig.3, when $A = 0.001$, the water content distribution is close to "L" shape, that is, in a small height range above groundwater, the water content drops rapidly to the surface water content; when $A = 0.050$, the water content above the groundwater level slowly decreases to the surface water content of the soil as the elevation increases. It can be seen that as the value A continues to increase, the water content along the elevation distribution curve gradually transitions from an "L" shape to a linear shape. According to the author's extensive test results (not listed here due to space limit), when the coarse grain of the soil increases and the soil type approaches sandy soil, A takes a smaller value, and when the clay particles in the soil increase, the water retention increases, and the soil type approaches clayey soil, A takes a larger value. It can be seen from Fig. 4 that as the groundwater level continues to increase, the water content at each height of the soil body also increases. Fig.5 shows the comparison between the predicted and the measured values of the initial water content distribution of different soil types along the elevation, from which we can see that the predicted change trend is consistent with the test results. Thus, it is feasible to use this

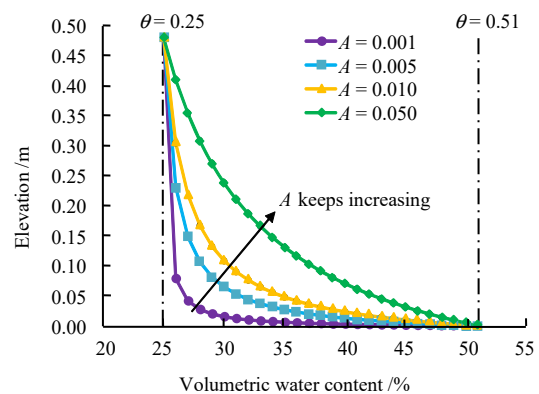


Fig.3 Effect of A value on the water content distribution

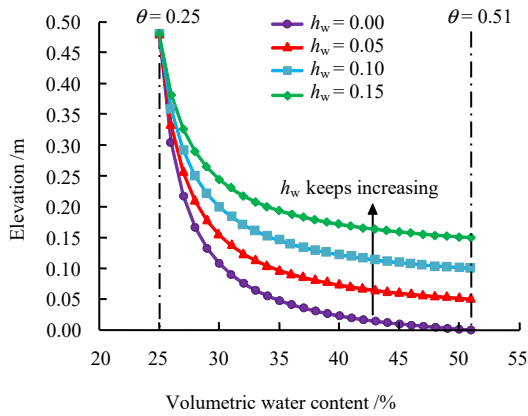


Fig.4 Effect of groundwater level on the water content distribution

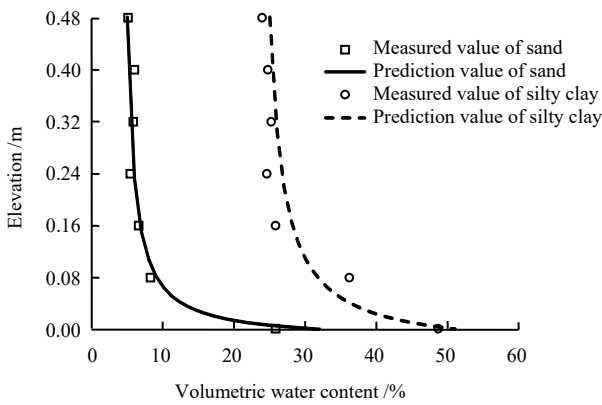


Fig.5 Comparison between the predicted and measured initial water contents of different soils

function to approximately describe the initial water content distribution of soil.

In order to obtain the variation characteristics of the initial water content along the elevation, the functional expression of the water content can be obtained by derivation of Eq. (1) in the reverse direction:

$$\left. \begin{aligned} \theta &= B - \lambda + A(h - h_w + \mu)^{-1} & h \in (h_w, H] \\ \theta &= \theta_s & h \in [0, h_w] \end{aligned} \right\} \quad (5)$$

3.2 Water content distribution during rainfall infiltration

By observing the test process, it can be seen that, during rainfall, when the rainfall intensity is less than the saturated permeability coefficient of the soil body, the permeability coefficient corresponding to the water content of the surface soil body is the same as the rainfall intensity, and the soil surface water content is in a dynamic equilibrium state. At the same time, studies have shown that the relationship between the permeability coefficient *k* of the soil and its water content can be expressed by the soil–water characteristic curve and permeability coefficient function of unsaturated soil^[13]

$$\theta(s) = \theta_r + (\theta_s - \theta_r) \left[1 + \left(\frac{s}{\alpha} \right)^n \right]^{-m} \quad (6)$$

where *s* is the matric suction; θ_s and θ_r are the saturated water content and residual water content of the soil, respectively; and *m* and *n* are the control parameters of the soil water characteristic curve.

$$k(s) = k_{sat} \frac{\left[1 - (as^{(n-1)}) \left(1 + (as^n)^{-m} \right) \right]^2}{1 + (as^n)^{\frac{m}{2}}} \quad (7)$$

where k_{sat} is the saturation permeability coefficient.

By eliminating the matrix suction terms in Eqs. (6) and (7), the function relationship between the water content of the top soil and the rainfall intensity under different rainfall intensities can be established as

$$\theta = f(k) \quad (8)$$

According to the above research, a simplified model of the distribution of soil water content along the elevation during rainfall infiltration can be obtained, as shown in Fig.6. It can be seen from this that during the process of rainfall infiltration, the soil surface water content continues to increase. As the rainfall duration continues, the rainfall infiltration depth $h_{\theta q}$ also gradually increases, and finally the infiltration rainwater reaches the groundwater level, causing the groundwater level to rise. Comparing the test results, we can see that the simplified model of water content distribution is consistent with the test results and has credibility. In the figure: the horizontal and vertical coordinates are the volumetric water content and elevation, respectively; θ_i is the initial water content of the soil, which has the same meaning as *B* in Eq. (2); θ_q is the soil water content when the rainfall intensity is *q*; $h_{\theta q}$ is the depth of infiltration.

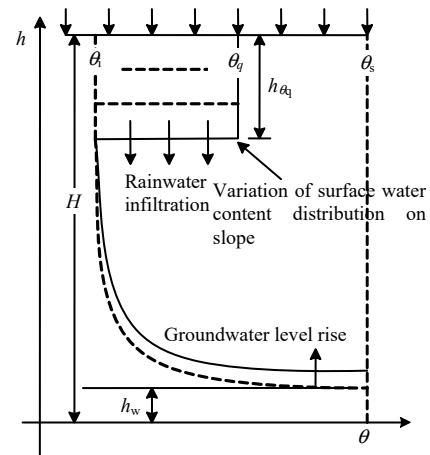


Fig.6 Distribution of soil water content during rainfall infiltration process

3.3 Drainage process of soil slope

Rainfall infiltration will cause the groundwater level inside the slope to rise and reduce the stability of the slope. However, in fact the groundwater level inside the slope does not continue to increase with the accumulation of rainfall, but continuously oozes out according to a certain pattern. After rainfall stopping, the groundwater level will drop, increasing the slope stability. Referring to the research results of Montrasio et al.^[14], according to Darcy's law, the drainage rate of the slope is proportional to the height of the groundwater level:

$$K_T \sin \beta h_w \cos \beta \Delta t = n_s \Delta h_w \cos \beta (1 - S_r) \quad (9)$$

where h_w is the groundwater level after time t seepage; K_T is the soil seepage capacity parameter; n_s is the soil porosity; S_r is the saturation; β is the slope; and t is the seepage time.

Therefore, from Eq. (9), the water table of the slope can be obtained:

$$\frac{\Delta h_w}{\Delta t} = h_w \frac{K_T \sin \beta}{n_s (1 - S_r)} \quad (10)$$

$$h_w(t) = h_{w0} e^{-K_T \frac{\sin \beta}{n_s (1 - S_r)} t} \quad (11)$$

where h_{w0} is the initial groundwater level.

Based on the inverse proportional model of the initial water content distribution, rainfall infiltration model and soil drainage model, the soil weight and shear strength changes of the slope during rainfall infiltration can be further studied, which provides a reliable basis for slope stability analysis.

4 Slope stability analysis based on water content distribution model

4.1 Shear strength of the unsaturated soil

Fredlund et al.^[15] firstly proposed that matric suction in unsaturated soil could improve its cohesion. The following formula can be used to express the effect of matrix suction on cohesion of unsaturated soil.

$$c = c' + (u_a - u_w) \tan \phi^b \quad (12)$$

where c is the total cohesive force; c' is the effective cohesive force; u_a is the pore gas pressure; u_w is the pore water pressure, generally $(u_a - u_w)$ can be regarded as the matrix suction; ϕ^b is suction-related friction angle. Vanapalli et al.^[16] proposed the following calculation method of ϕ^b :

$$\tan \phi^b = \left(\frac{\theta - \theta_r}{\theta_s - \theta_r} \right) \tan \phi \quad (13)$$

The matrix suction in Eq. (12) can be inferred from the expression of the soil–water characteristic curve shown in Eq. (6):

$$u_a - u_w = \frac{\left[\left(\frac{\theta_s - \theta_r}{\theta - \theta_r} \right)^{1/m} - 1 \right]^{1/n}}{\alpha} \quad (14)$$

It can be seen from the above analysis that the change of the cohesive force of the soil can be expressed as a function of the water content. Therefore, substituting Eq. (14) into Eq. (12) will obtain the slope cohesion along the elevation direction during rainfall. Since the friction angle in the soil changes only slightly with the water content^[17], it is considered that the friction angles in the soil at all elevations are the same, and the shear strength inside the slope can be determined.

4.2 Calculation method of slope stability

In order to simplify the slope stability calculation, the sliding surface is considered to be a straight-line segment, and the model is established by ignoring the forces between the soil slices at each position, as shown in Fig.6. Considering the distribution model of the slope water content and the unsaturated shear strength, the calculation method of slope stability coefficient F_s can be obtained as

$$F_s = T_s / T_d \quad (15)$$

$$T_d = W' \sin \beta + F' \quad (16)$$

$$T_s = N' \tan \phi + c \quad (17)$$

$$W' = \cos \beta \Delta s \gamma_w \cdot$$

$$\left[G_s (1 - n_s) H + h_q S_{rq} n_s + \left(\int_{h_w}^{H-h_q} \theta dh \right) - h_w (1 - n_s) \right] \quad (18)$$

$$\int_{h_w}^{H-h_q} \theta dh = (B - \alpha) (H - h_q - h_w) + A \ln \left(\frac{H - h_q - h_w}{\beta} + 1 \right) \quad (19)$$

$$F' = \gamma_w \sin \beta \cos \beta h_w \Delta s \quad (20)$$

$$N' = W' \cos \beta \quad (21)$$

where T_s and T_d are the anti-sliding force and sliding force at the designated sliding surface, respectively; W' is the submerged unit weight of the soil; β is the inclination of the sliding surface consistent with the slope inclination in Eq. (9); F' is the seepage force in the saturated area; N' is the normal force on sliding surface; Δs is the width of the bottom of the strip; γ_w is the water gravity; G_s is the specific gravity of soil particle; h_q is the height of the surface water content increase area caused by rainfall; S_{rq} is the saturation of the water content increase area caused by rainfall; h_s is the height of the sliding surface. The action point and direction of each parameter are shown in Fig.7.

5 Case studies

5.1 Project details

The Hang-Xin-Jing Expressway Qili connecting line is

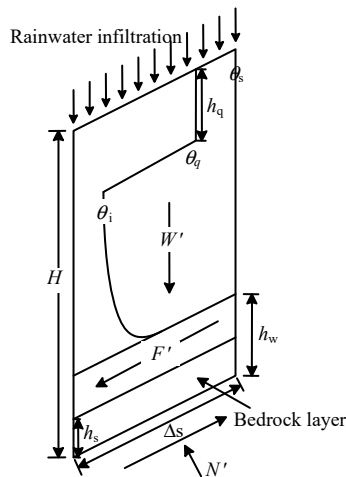


Fig.7 Distribution and force diagram of the slope water content under rainfall condition

located in the middle-low mountainous area of western Zhejiang. The maximum elevation of the mountain is 1050 m, and the connecting line elevation is 437–635 m. The section K5+400–K7+200 has steep terrain. The cohesive soil debris accumulated on the upper slope is composed of calcareous mudstone, mudstone, carbonaceous mudstone, marl, etc. The rock mass at the site has poor integrity due to strong tectonism. During the excavation of the cutting, some slopes were obviously cracked, and the shallow sliding of the slope surface of the slope #10 has caused severe deformation of the overlying frame beam, as shown in Fig.8.



Fig.8 A shallow landslide at the construction site

Based on the field geology and rainfall conditions, the above-mentioned water content distribution model and slope stability calculation method were used for stability analysis.

According to the on-site geological survey data and laboratory test results, the slope geometric parameters are shown in Table 2, and the stability calculation parameters are shown in Table 3, where the drainage parameter K_T value refers to the existing research results^[14]. The rainfall calculation data are taken from the field monitoring values from January 23 to May 12, 2016, in a total of 111 days.

Table 2 Geometries of the engineering slope

Slope soil type	Calculated total height of slope /m	Bedrock thickness /m	Inclination of slope /($^{\circ}$)	Initial groundwater level /m
Silty clay	5	0.5	25	0, 0.1, 0.2, 0.3

5.2 Influence of sliding surface on slope stability

Figure 9 shows the variation of slope stability coefficient with the height of the sliding surface from the bottom surface under different rainfall time conditions. It can be seen from this that under different rainfall times, the stability coefficients of different sliding surfaces of the slope increase with the increase of the sliding surface height. It can be inferred that at any moment of rainfall, the most dangerous sliding surface of the slope is located at 0.5 m from the bottom, i.e., the boundary of slope soil to bedrock. However, in the range of 0.5 m above the bottom of the model, it is moderately weathered rock, which has high shear strength and is not prone to instability. Therefore, in the subsequent analysis, the slope stability coefficients are corresponding to the sliding surface at 0.5 m from the bottom bedrock.

5.3 Influence of water content distribution parameters on slope stability

Figure 10 shows the effect of different water content distribution parameters A on the slope stability under the same rainfall conditions. It can be seen from Fig. 10(a) that when $A = 0.001$, the initial slope stability coefficient is 3.0, and as the rainfall continues, it basically remains unchanged; and when the rainfall reaches 80 d, the stability coefficient quickly decreases to 1.2, then remained stable(see Fig.10(b)). When $A = 0.005$, the initial stability coefficient is 3.0; during the subsequent rainfall, the stability coefficient fluctuates slightly with the change of rainfall intensity, and the stability coefficient drops to 1.2 after 80 days of rainfall. When $A = 0.010$, the initial slope stability coefficient is 2.8, and in the subsequent rainfall process, the stability coefficient changes significantly with the change of

Table 3 Soil parameters of the engineering slope

Porosity	Specific gravity of soil particles	Natural saturation	Water content distribution parameter	Drainage parameters /d ⁻¹	Total cohesion /kPa	Internal friction angle /($^{\circ}$)	m	n	α
0.51	2.7	0.5	0.001, 0.005, 0.010, 0.050	0.025 92	21	20	0.29	1.4	0.2

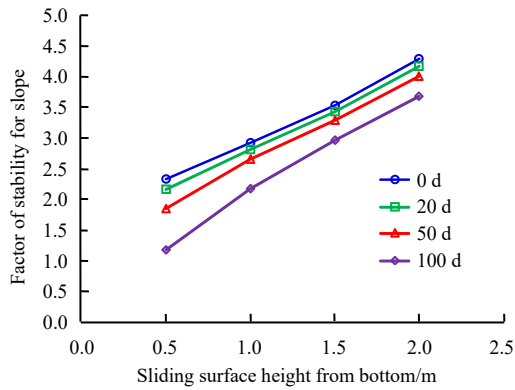


Fig.9 Slope stability at different sliding surfaces under the same rainfall intensity

rainfall intensity (see Fig.10(c)). When $A = 0.050$, the initial stability factor is 2.3, and it changes significantly with the change of rainfall intensity. Comprehensive analysis of the above results shows that a decrease in the water content distribution parameter A will increase the initial stability of the slope and gradually weaken due to the impact of rainfall intensity changes, but when the cumulative rainfall reaches a certain level, the stability coefficient suddenly decreases. If the value of A keeps increasing, the initial stability of the slope will decrease, and the

influence of rainfall intensity will become more and more obvious.

The main reason for the above phenomenon is that when A is small, the water retention capacity of the soil is weakened, and the water content of the part above the groundwater level is rapidly reduced, which leads to the obvious difference in the cohesive force of the soil above and below the groundwater level. Therefore, the slope stability coefficient is significantly affected by the groundwater level. When A is large, there is a clear transition between the groundwater level and the water content of the slope surface, and the change of the soil cohesion will not be a sudden but a gradual change, thereby the slope stability coefficient is less affected by rainfall (as shown in Fig. 10(d)).

5.4 Effect of groundwater level on rainfall intensity-duration curve of slope

In the analysis and prediction of slope stability, the rainfall intensity-duration curve (I-D curve) is the most commonly used prediction method, that is, taking the slope instability as the standard, the relationship between rainfall intensity and rainfall duration is counted. Previous studies have shown that the rainfall duration curve is closely related to the local soil type, slope shape, initial conditions, etc.^[18], and the groundwater

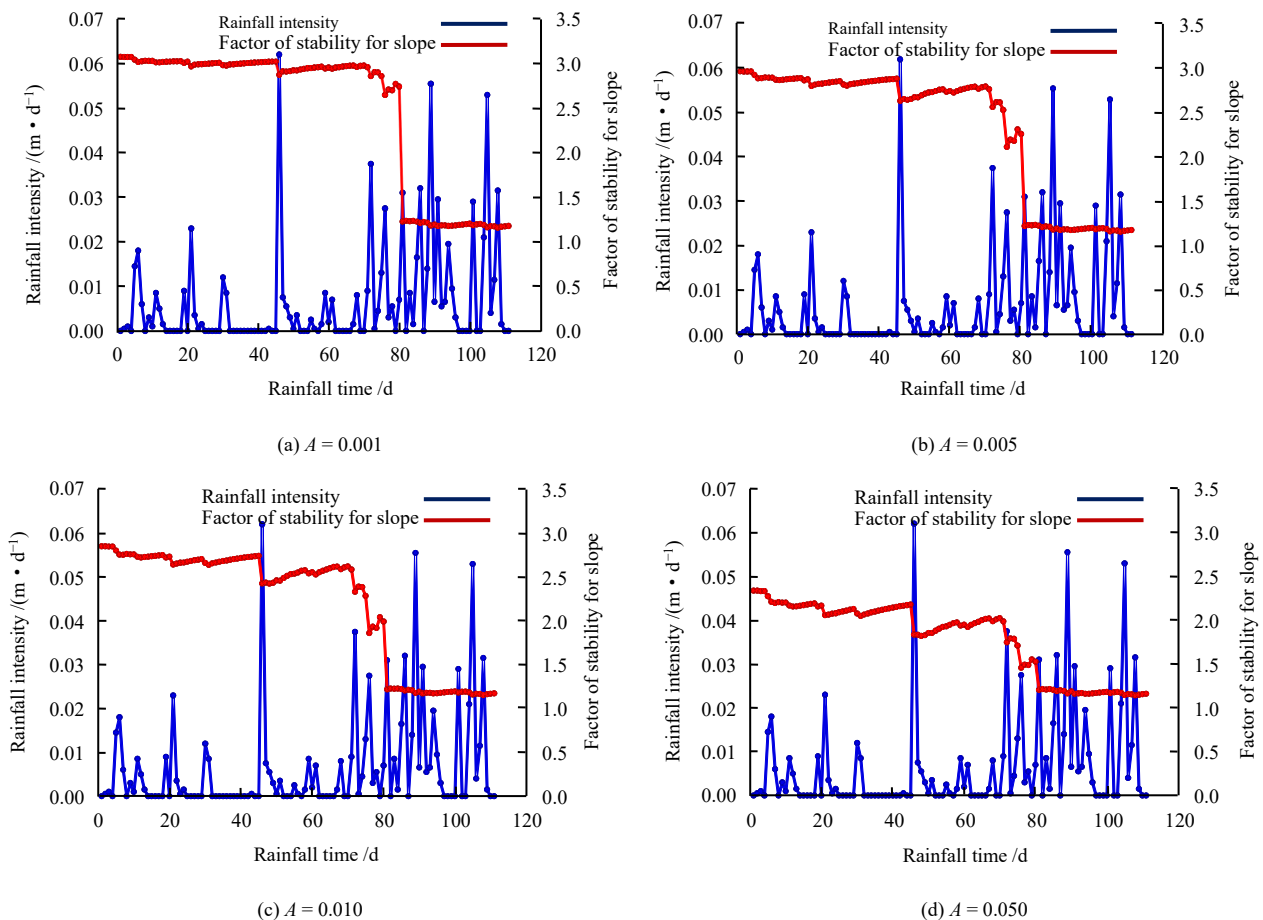


Fig.10 Slope stability under different water content distribution parameters

level is one of the most obvious factors. Therefore, it is of great significance to analyze the changes of slope stability with rainfall intensity and rainfall duration under different groundwater levels.

Since the rainfall duration curve is to analyze the slope stability under average rainfall conditions, we can set the rainfall intensity to be 2, 5, 10, 50 mm/h constantly while increasing the rainfall time to obtain the change trend of slope stability. As shown in Fig.11, comparing the stability of the initial state of the slope under different groundwater levels, it can be seen that when the groundwater level are 0, 0.1, 0.2, and 0.3 m, the initial stability coefficients of the slope are 2.33, 2.21, 2.08, and 1.91, respectively, namely, the initial slope stability

coefficient presents a downward trend as the initial groundwater level rises. Comparing the changes of slope stability in different rainfall conditions, we can see that under the same rainfall intensity, the higher the initial water level, the shorter the time required for the slope stability to decrease to 1.3, and the decline of stability is small in the early period of rainfall and increases rapidly in the later period; Under the same rainfall time condition, the higher the initial water level, the smaller the rainfall intensity required to reduce the slope stability coefficient to 1.3.

Figure 12 shows a comparison of the rainfall intensity-duration curve^[19] of slopes in the project area and slopes in other areas under different groundwater levels. It can

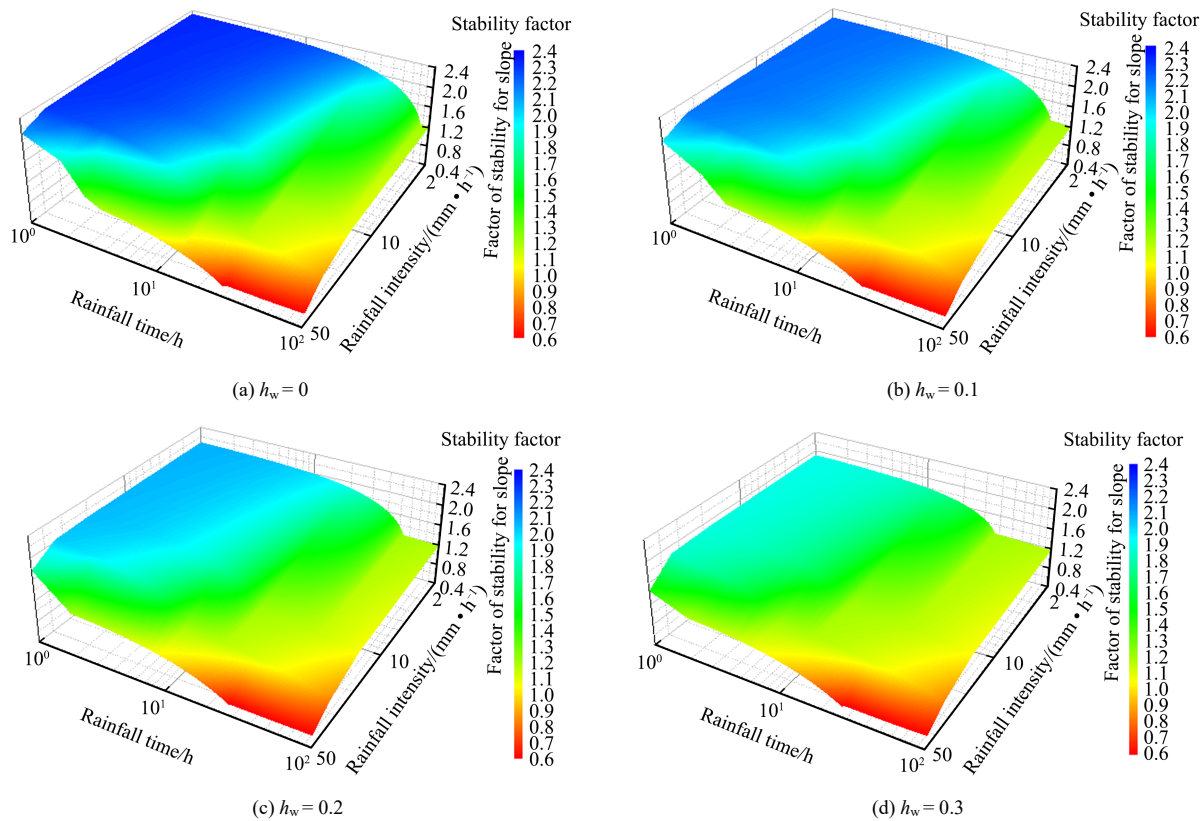


Fig.11 Relationship between the slope stability and rainfall intensity-duration under different groundwater level conditions

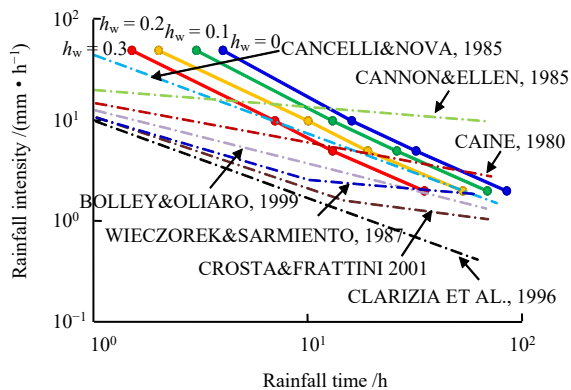


Fig.12 Rainfall intensity-duration curves of slopes in the engineering area and other places^[19]

be seen that when the rainfall intensity is the same, the rainfall time required for the slope to reach instability decreases with increasing groundwater level. When the rainfall time is the same, the rainfall intensity required for the slope to reach instability decreases as the groundwater level increases. In general, a higher initial groundwater level would induce more instability of the soil slope, and vice versa.

6 Conclusions

According to the test results, the distribution of the initial water content of the soil along the elevation could be expressed by an inverse proportional function, and the water distribution parameter A , correction coefficients λ and μ were introduced to

characterize the distribution of different types of soils. It was found that a larger the value of A , the closer the soil is to clay, and the better the water retention capacity; in contrast, the smaller value of A indicated the soil is closer to sand and the water retention capacity is worse.

In the process of rainfall infiltration, the change of the internal water content of the soil has the following trend: in the case of inverse proportional distribution of the initial water content, as the rainfall continues, the surface water content of the soil gradually rises to a certain value, and then the internal water content of the soil increases from top to the bottom; when rainfall infiltrates the bottom of the soil, the groundwater level gradually rises from bottom to top until the soil is fully saturated.

According to the distribution characteristics of water content in the process of rainfall infiltration, a method for calculating the stability of soil slope was proposed. The calculation results showed that the slope stability would decrease as the rainfall continues. After the rainfall stopped, the stability would gradually increase. The closer the sliding surface is to the bottom of the slope, the smaller the slope stability coefficient.

At last, it was found that the smaller the water content distribution parameter A , the more sensitive the slope stability to the rainfall response; the larger the water content distribution parameter A , the smaller the slope stability is affected by rainfall. Also, the rainfall intensity-duration curve is greatly affected by the initial groundwater level of the slope: high initial groundwater level tends to induce slope instability under the influence of rainfall infiltration.

Reference

- [1] ZHANG Jian, LI Jiang-teng, LIN Hang, et al. Delay phenomenon of shallow slope failure triggered by rainfall and its correlation with soil parameters[J]. *Journal of Central South University (Science and Technology)*, 2018, 49(1): 150–157.
- [2] WANG Hao, WANG Ming-zhe, CHEN Xiu-jun, et al. Analysis and discussion on the mechanism of multiple sliding for cutting high slope during construction[J]. *The Chinese Journal of Geological Hazard and Control*, 2016(3): 14–21.
- [3] ZHAN Qun, XU Qiang, YI Jing-song, et al. Rainfall infiltration depth and formation mechanism of slow-inclination soil landslides in Nanjiang[J]. *Chinese Journal of Geotechnical Engineering*, 2016, 38(8): 1447–1455.
- [4] FU Hong-yuan, SHI Zhen-ning, QIU Xiang, et al. Seepage and Deformation Test of Carbonaceous Mudstone-soil Layered Embankment Under Water Immersion[J]. *China Journal of Highway and Transport*, 2017, 30(11): 1–8, 98.
- [5] MA Ji-qian, FU Hong-yuan, WANG Gui-yao, et al. Seepage characteristics of layered soil slope under rainfall conditions[J]. *Journal of Central South University (Science and Technology)*, 2018, 49(2): 464–471.
- [6] ZENG L, BIAN H B, SHI Z N, et al. Forming condition of transient saturated zone and its distribution in residual slope under rainfall conditions[J]. *Journal of Central South University*, 2017, 24(8): 1866–1880.
- [7] FU Hong-yuan, MA Ji-qian, SHI Zhen-ning, et al. Key Issues and Research Progress of Shear Strength Theory of Unsaturated Soil[J]. *China Journal of Highway and Transport*, 2018, 31(2): 1–14.
- [8] SHI Zhen-ming, ZHAO Si-yi, SU Yue. An experimental study of the deposit slope failure caused by rainfall[J]. *Hydrogeology & Engineering Geology*, 2016, 43(4): 135–140.
- [9] ZUO Zi-bo, ZHANG Lu-lu, WANG Jian-hua. Model tests on rainfall-induced colluvium landslides: effects of particle-size distribution[J]. *Chinese Journal of Geotechnical Engineering*, 2015, 37(7): 1319–1327.
- [10] TIAN Dong-fang, ZHENG Hong, LIU De-fu. 2D FEM numerical simulation of rainfall infiltration for landslide with considering runoff effect and its application[J]. *Rock and Soil Mechanics*, 2016, 37(4): 1179–1186.
- [11] WANG Ding-jian, TANG Hui-ming, LI Chang-dong, et al. Stability analysis of colluvial landslide due to heavy rainfall[J]. *Rock and Soil Mechanics*, 2016, 37(2): 439–445.
- [12] CUOMO S, DELLA SALA M. Rainfall-induced infiltration, runoff and failure in steep unsaturated shallow soil deposits[J] *Engineering Geology*, 2013: 118–127.
- [13] VAN GENUCHTEN M T. A Closed-form Equation for Predicting the Hydraulic Conductivity of Unsaturated Soils[J]. *Soil Science Society of America Journal*, 1980, 44(5): 892–898.
- [14] MONTRASIO L, VALENTINO R. A model for triggering mechanisms of shallow landslides[J]. *Natural Hazards and Earth System Sciences*, 2008, 8(5): 1149–1159.
- [15] FREDLUND D G, MORGENSTERN N R, WIDGER R A. The shear strength of unsaturated soils[J]. *Canadian Geotechnical Journal*, 1978, 15(3): 313–321.
- [16] VANAPALLI S K, FREDLUND D G, PUF AHL D E, et al. Model for the prediction of shear strength with respect to soil suction[J]. *Canadian Geotechnical Journal*, 1996, 33(3): 379–392.
- [17] HUANG Kun, WAN Jun-wei, CHEN Gang, et al. Testing study of relationship between water content and shear strength of unsaturated soils[J]. *Rock and Soil Mechanics*, 2012, 33(9): 2600–2604.
- [18] ZHAN Liang-tong, LI He, CHEN Yun-min, et al. Parametric analyses of intensity-duration curve for predicting rainfall-induced landslides in residual soil slope in Southeastern coastal areas of China[J]. *Rock and Soil Mechanics*, 2012, 33(3): 872–880.
- [19] GUZZETTI F, PERUCCACCI S, ROSSI M, et al. Rainfall thresholds for the initiation of landslides in central and southern Europe[J]. *Meteorology & Atmospheric Physics*, 2007, 98(3–4): 239–267.